CHAPTER IV
RESULTS AND DISCUSSION

4.1 Catalyst Characterization

Table 4.1 Textural properties of the prepared catalysts

Catalyst	Label	BET Surface (m^2/g)	Total Pore Volume (cm^3/g)	Average Pore Diameter (nm)
$Ce_{0.75}Zr_{0.25}O_2$ (SG*)	CZO-S	97	0.10	7.4
$Ce_{0.75}Zr_{0.15}Mn_{0.1}O_2$	CZN-1	87	0.14	7.2
$Ce_{0.75}Zr_{0.05}Mn_{0.2}O_2$	CZN-2	85	0.17	6.9
$15Ni/Ce_{0.75}Zr_{0.25}O_2$ (SG*)	Ni/CZO-S	78	0.09	6.7
$15Ni/Ce_{0.75}Zr_{0.15}Mn_{0.1}O_2$	Ni/CZN-1	68	0.13	6.6
$15Ni/Ce_{0.75}Zr_{0.05}Mn_{0.2}O_2$	Ni/CZN-2	64	0.15	6.2
$Ce_{0.75}Zr_{0.25}O_2$ (CP**)	CZO-C	156	0.34	12.0
$Ce_{0.75}Zr_{0.15}Mg_{0.2}O_2$	CZM-1	154	0.32	11.7
$Ce_{0.75}Zr_{0.05}Mg_{0.4}O_2$	CZM-2	133	0.25	11.1
$15Ni/Ce_{0.75}Zr_{0.25}O_2$ (CP**)	Ni/CZO-C	138	0.31	10.8
$15Ni/Ce_{0.75}Zr_{0.15}Mg_{0.2}O_2$	Ni/CZM-1	124	0.29	10.1
$15Ni/Ce_{0.75}Zr_{0.05}Mg_{0.4}O_2$	Ni/CZM-2	115	0.18	9.8

*SG=Sol-Gel.

** CP= Co-Precipitation

4.1.1 Textural Properties

Table 4.1 summarizes the textural properties of the prepared catalysts. The results showed that the CZO-S and CZNs are in range of 85-97 m^2/g, total pore volumes of 0.10-0.17 cm^3/g and average pore diameters 6.9-7.4 nm (Bampenrat *et al.*, 2010). The surface area of CZO-C and CZM are in range of 133-156 m^2/g, total pore volumes of 0.25-0.34 cm^3/g and average pore diameters 11.1-12.0 nm, which

are higher than those of CZO-S and CZNs supports. It can be noted that the higher surface area and total pore volume cause preparation method. The surface areas decreased approximately 11-25 % when impregnated with Ni onto those supports, due to the pore blockage of nickel species (Chen *et al.*, 2008). It is apparent that the Ni/CZO prepared by co-precipitation yielded higher surface area and total pore volume than Ni/CZO prepared by sol-gel method. The incorporation of Mn or Mg into the support caused the surface area of its parent catalyst to reduce in relation to its incorporated amount. This might be because of the differences in morphology as evidenced by SEM.

4.1.2 Temperature-Programmed Reduction of Hydrogen (H_2-TPR)

The reducibility of the supports and catalysts evaluated by H_2-TPR is shown in Figures 4.1 and 4.2.

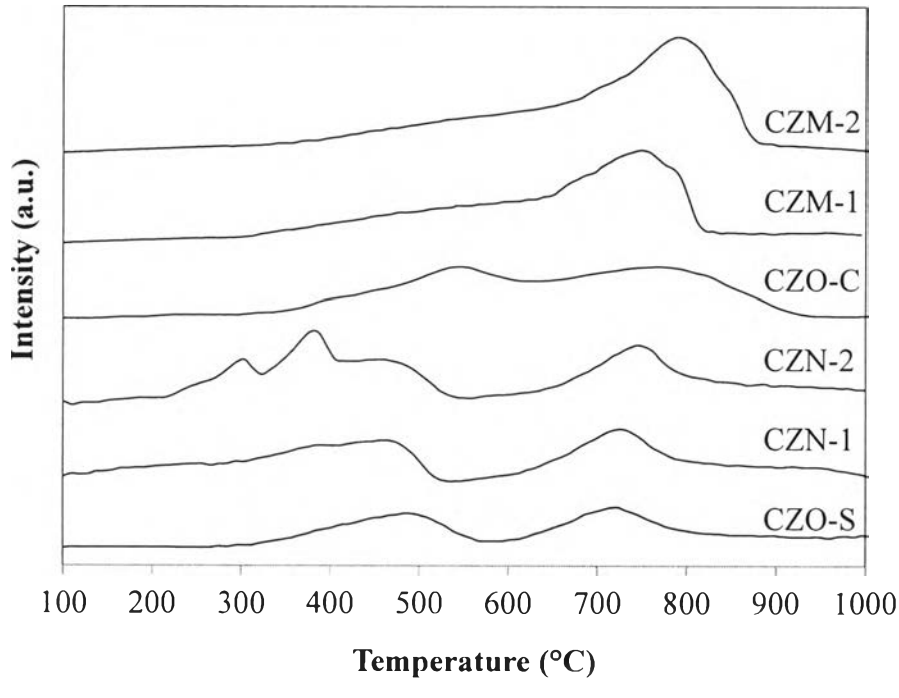

Figure 4.1 H_2-TPR profiles for supports with a heating rate of 10 °C/min, a reducing gas containing 5 % H_2 in Ar with a flow rate of 50 ml/min.

The results showed that the reducibility of supports prepared by sol-gel method (CZN-1, CZN-2, and CZO-S,) are better than other ones, prepared by

co-precipitation method (CZM-1, CZM-2, and CZO-C) indicating by lower temperature reduction.

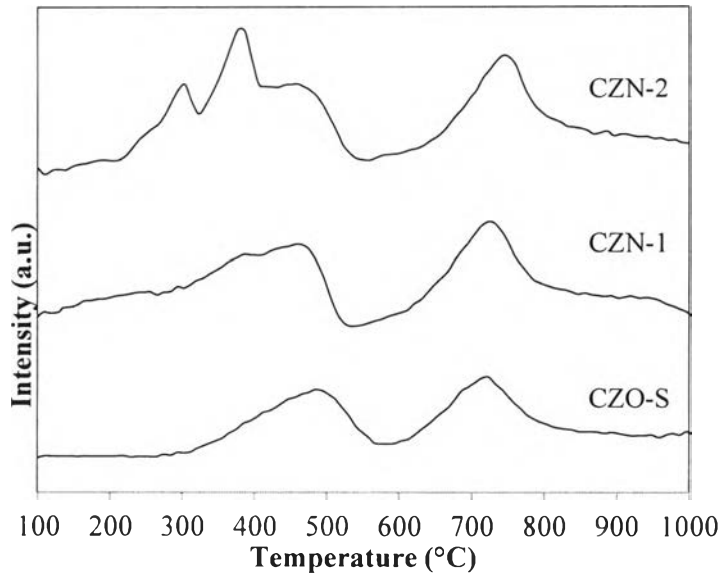

Figure 4.2 H_2-TPR profiles for Mn-doped supports, prepared by sol-gel method, with a heating rate of 10 °C/min, a reducing gas containing 5 % H_2 in Ar with a flow rate of 50 ml/min.

In Figure 4.2, TPR profiles of Mn-doped supports prepared by sol-gel method were found that CZO-S support exhibited a typical reduction peaks at ca. 500 °C and ca. 720 °C which correspond to surface reduction and bulk reduction of cerium oxide, respectively (Pengpanich *et al.*, 2004). However, two similar peaks were observed as CZN-1 support at ca. 460 °C and 720 °C, respectively. The decreasing reduction temperature resulted from the Mn incorporation suggested that manganese cations dissolve in the ceria lattice (Tang *et al.*, 2006). Moreover, as Mn loading was further increased; CZN-2, one could observe the shoulder reduction peak at ca. 210-270 °C attributed to the readily reducible small cluster surface manganese species, i.e., the reduction of MnO_2 to Mn_2O. The peaks appearing in the two temperature ranges of 270-320 °C and 320-410 °C were ascribed to the reduction of MnO_2/Mn_2O_3 to Mn_3O_4, and of Mn_3O_4 to MnO, respectively (Wu *et al.*, 2007). Interestingly, the reduction temperature of surface oxygen of cerium oxide

was shifted to a lower temperature of ca. 100 °C when Mn was incorporated into the mixed oxides. This suggests that the reducibility of cerium oxide be promoted, probably due to the formation of solid solution between the manganese and cerium oxides resulting in the enhancement of oxygen mobility (Bampenrat *et al.*, 2010).

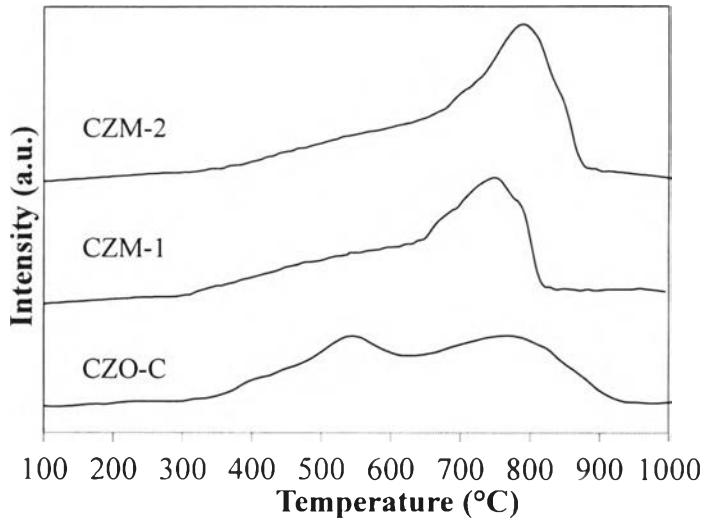

Figure 4.3 H_2-TPR profiles for Mg-doped supports, prepared by co-precipitation method, with a heating rate of 10 °C/min, a reducing gas containing 5 % H_2 in Ar with a flow rate of 50 ml/min.

Figure 4.3 shows all TPR profiles of Mg-doped supports prepared by co-precipitation method. The TPR profile for CZO-C indicated typical reduction peaks at ca. 530 °C and ca. 790 °C which correspond to surface reduction and bulk reduction of cerium oxide, respectively. The CZM-1 exhibited a reduction peak at 750 °C, the shoulder reduction peak at ca. 300-600 °C attributed to the reducibility of cerium oxide. The CZM-2 showed a reduction peak at ca. 800 °C, the shoulder reduction peak of cerium oxide at ca. 350-600 °C. The results showed that the CZM-1 had lower reducibility shoulder reduction peak of cerium oxide than the CZM-2 and CZO-C. This suggests that the reducibility of cerium oxide was enhanced when Mg-incorporated supports at lower temperatures, however, the higher amount of Mg-added support increased reduction temperatures at high temperature.

This is a result from formation of solid solution between the manganese and cerium oxides resulting in the enhancement of oxygen mobility.

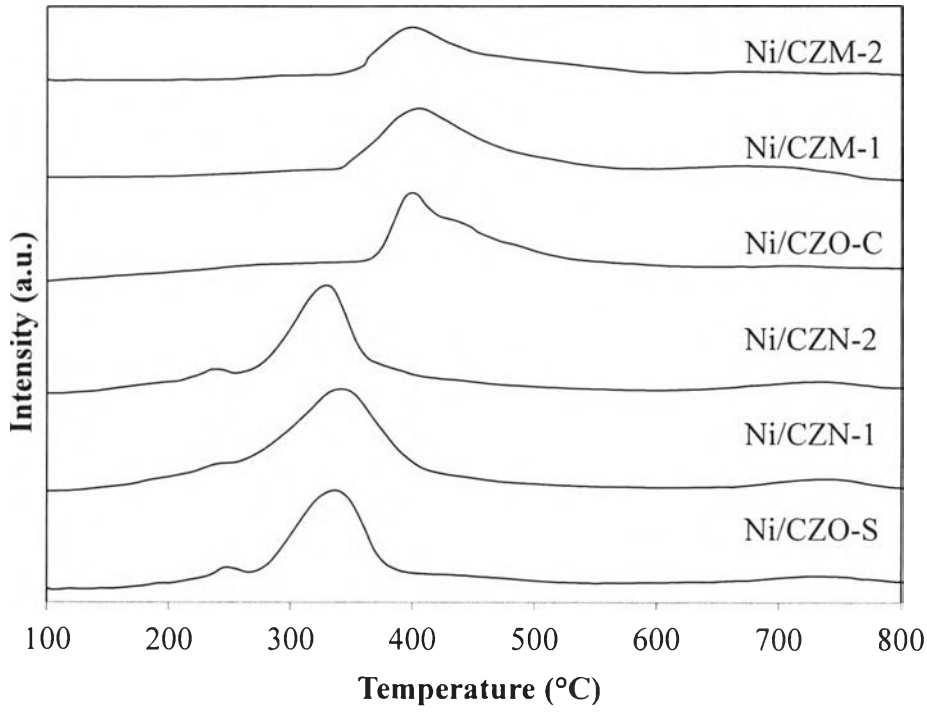

Figure 4.4 H_2-TPR profiles for catalysts with a heating rate of 10 °C/min, a reducing gas containing 5 % H_2 in Ar with a flow rate of 50 ml/min.

Figure 4.4 showed the H_2-TPR profiles of the catalysts, indicating that two H_2 consumption peaks are clearly observed for the catalysts prepared by sol-gel method; Ni/CZO-S, Ni/CZN-1 and Ni/CZN-2. The low temperature peak in the range of 230-270 °C can be associated with the reduction of free NiO particles and the other peak in the range of 270-400 °C can be ascribed to the reduction of complex NiO species in intimate contact with the oxide support (Bampenrat *et al.*, 2001). In case of the catalysts prepared by co-precipitation method; Ni/CZO-C, Ni/CZM-1 and Ni/CZM-2, a broad peak attributed to agglomerated Ni is observed from 350 °C to 600 °C. The higher temperature reduction was indicative of a strong interaction occurring between Ni and support. The Mg-containing catalysts had higher reduction temperature than the Mn-containing catalyst. It is suggested that

there were relatively strong interactions between NiO and Mg-doped support resulting in a more difficulty for the reducibility of the catalysts.

4.1.3 X-ray Diffraction (XRD)

The X-ray diffraction patterns of different $Ce_{0.75}Zr_{0.25-x}Mn_xO_2$ (CZN) mixed oxide and catalyst impregnated with 15%Ni (Ni/CZN) are presented in Figure 4.6. It was found that all catalysts exhibit major peaks at ca. 28.8°, 33.5°, 47.5°, and 56.8° (2θ) indicating the cubic fluorite structure of CeO_2. Several small peaks characteristic of NiO are observed at ca. 37°, 43° and 62° (2θ). No peak of either zirconia or manganese oxides is observed indicating that all zirconium cations and manganese cations dissolve in the ceria lattice. The results are similar to Bapenrat *et al.* (2010).

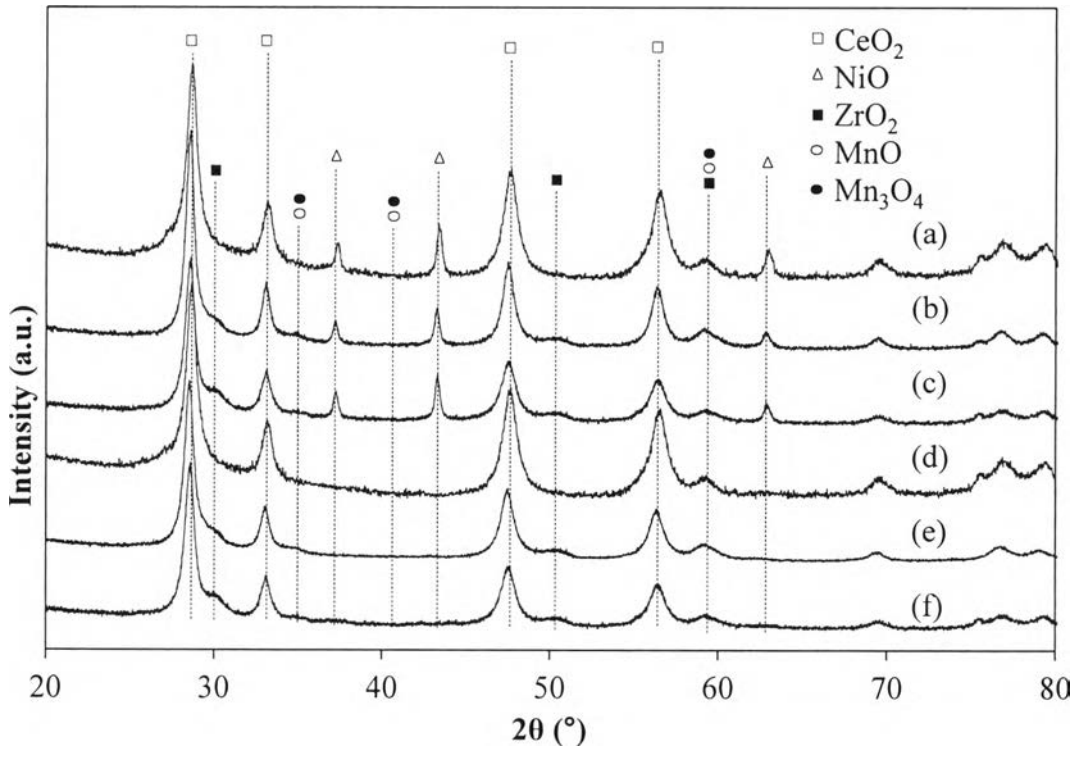

Figure 4.5 XRD patterns of the catalysts: (a) $Ce_{0.75}Zr_{0.25}O_2$ (CZO-S), (b) $Ce_{0.75}Zr_{0.15}Mn_{0.1}O_2$ (CZN-1), (c) $Ce_{0.75}Zr_{0.05}Mn_{0.2}O_2$ (CZN-2), (d) 15Ni/$Ce_{0.75}Zr_{0.25}O_2$ (Ni/CZO-S), (e) 15Ni/$Ce_{0.75}Zr_{0.15}Mn_{0.1}O_2$ (Ni/CZN-1), (f) 15Ni/$Ce_{0.75}Zr_{0.05}Mn_{0.2}O_2$ (Ni/CZN-2).

XRD patterns for all of the catalysts are shown in Figure 4.7. All the catalysts exhibited major peaks at ca. 28.8°, 33.5°, 47.5°, and 56.8° (2θ) representing the indices of (111), (200), (220) and (311) planes indicating a cubic fluorite structure of CeO_2 (Pengpanich *et al.*, 2002; Xu, S and Wang, X., 2005). Small peaks of NiO were observed at ca. 37.9°, 43.3°, and 62.7° (2θ) which is in good agreement with that reported by Bampenrat *et al.* (2010). No distinguishable peaks of MgO could be observed for the catalysts prepared. This indicated the incorporation of Mg into the ceria-zirconia lattices and/or the small amount of Mg residing in the catalyst. The NiO particle sizes calculated from the Scherer's equation for the Ni-doped catalysts were ca. 27-30 nm.

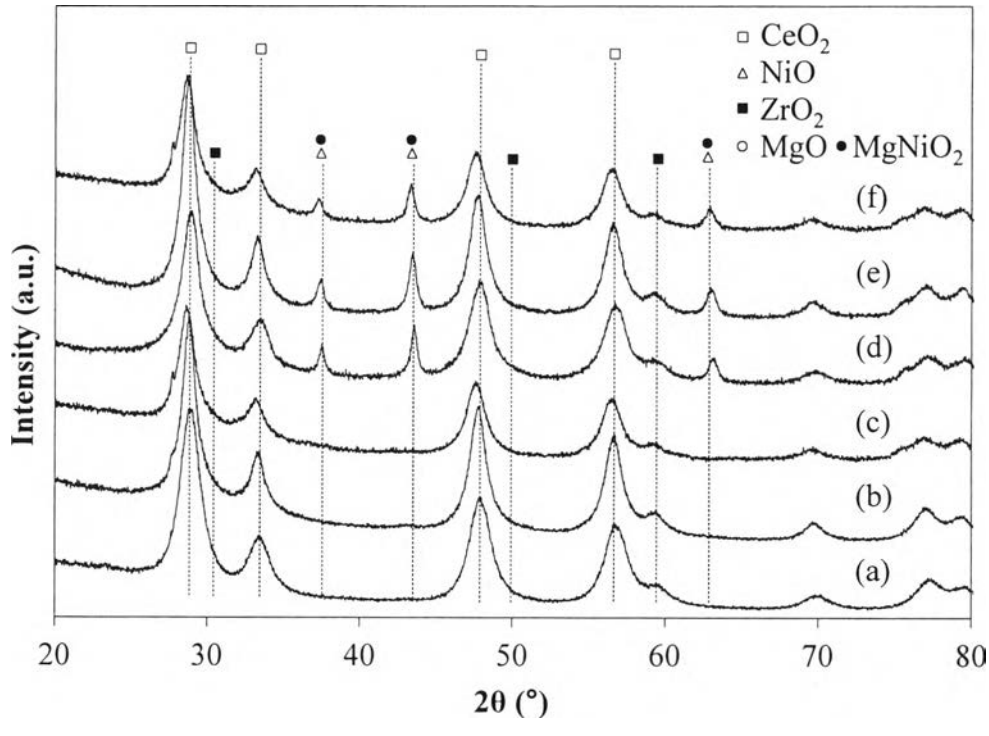

Figure 4.6 XRD patterns of the catalysts: (a) $Ce_{0.75}Zr_{0.25}O_2$ (CZO-C), (b) $Ce_{0.75}Zr_{0.15}Mg_{0.2}O_2$ (CZM-1), (c) $Ce_{0.75}Zr_{0.05}Mg_{0.4}O_2$ (CZM-2), (d) $15Ni/Ce_{0.75}Zr_{0.25}O_2$ (Ni/CZO-C), (e) $15Ni/Ce_{0.75}Zr_{0.15}Mg_{0.2}O_2$ (Ni/CZM-1), (f) $15Ni/Ce_{0.75}Zr_{0.05}Mg_{0.4}O_2$ (Ni/CZM-2).

4.1.4 Temperature-Programmed Desorption of Ammonia (NH_3-TPD)

Temperature programmed desorption of NH_3 was used to investigate the strength of acid sites. The acidic strength of the sites was determined according to the temperature at which ammonia is desorbed. Likewise the area obtained for each support is directly related to the amount of total acidity. Figure 4.8 shows the NH_3-TPD profile of prepared mixed oxide supports. The CZOs and CZNs supports show that there are two desorption peaks at 100 °C and 340 °C, which are attributed to the desorption ammonia of weak and medium acidic strength, respectively. The first peak at high amount of desorbed ammonia is assigned to weak acid sites in the temperature range of ca. 30-250 °C. The high temperature in peak can be assigned to medium acid sites the range of ca. 250-500 °C. In contrast, the first peak of CZM shifts to a lower temperature of ca. 70 °C when increasing Mg content. The acidity of supports determines from TPD peak area decreased in the order of CZN-2 > CZN-1 > CZO-C > CZO-S > CZM-1 > CZM-2.

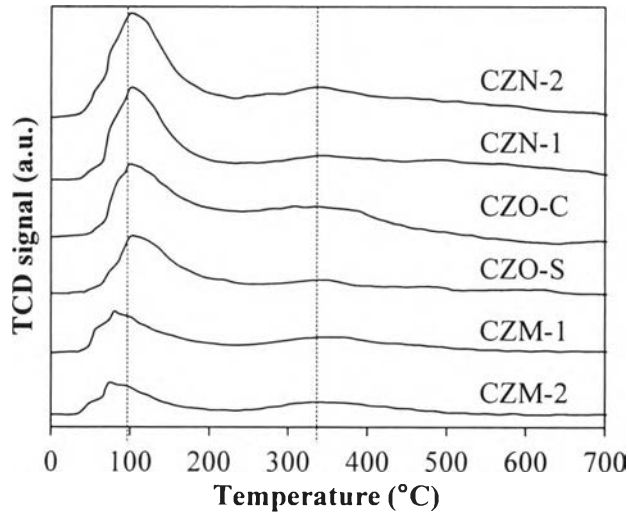

Figure 4.7 NH_3-TPD profiles of various mixed oxide supports.

4.1.5 Scanning Electron Microscopy (SEM)

Figure 4.9 shows SEM images of all the catalysts investigated. For the supports, both the modified and unmodified CZO present a similar morphology of the ceria-zirconia mixed oxide.

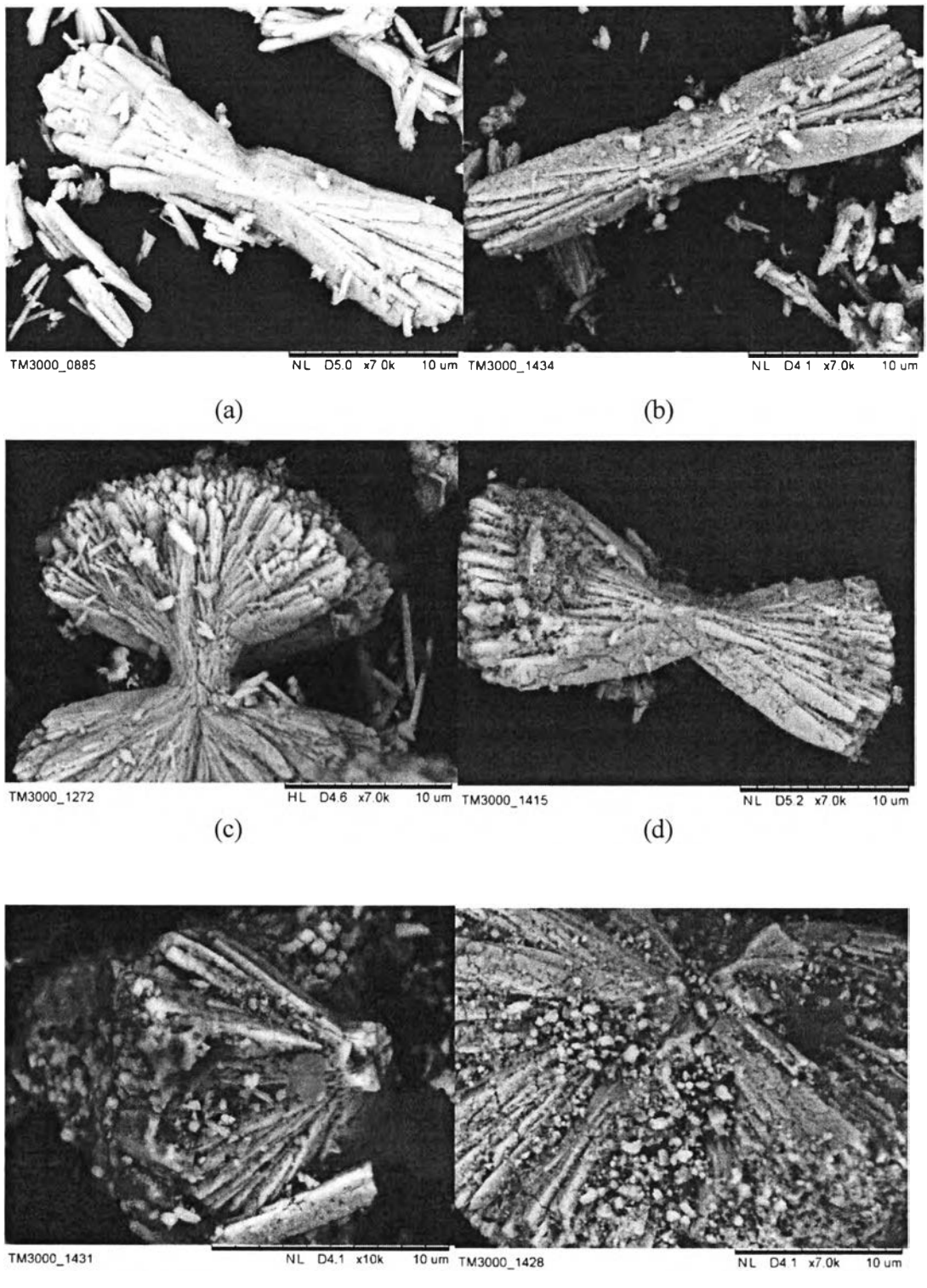

Figure 4.8 SEM images (7000-10000x magnifications) of a) CZO-S, b) Ni/CZO-S, c) CZN-1 d) Ni/CZN-1, e) CZN-2, f) Ni/CZN-2.

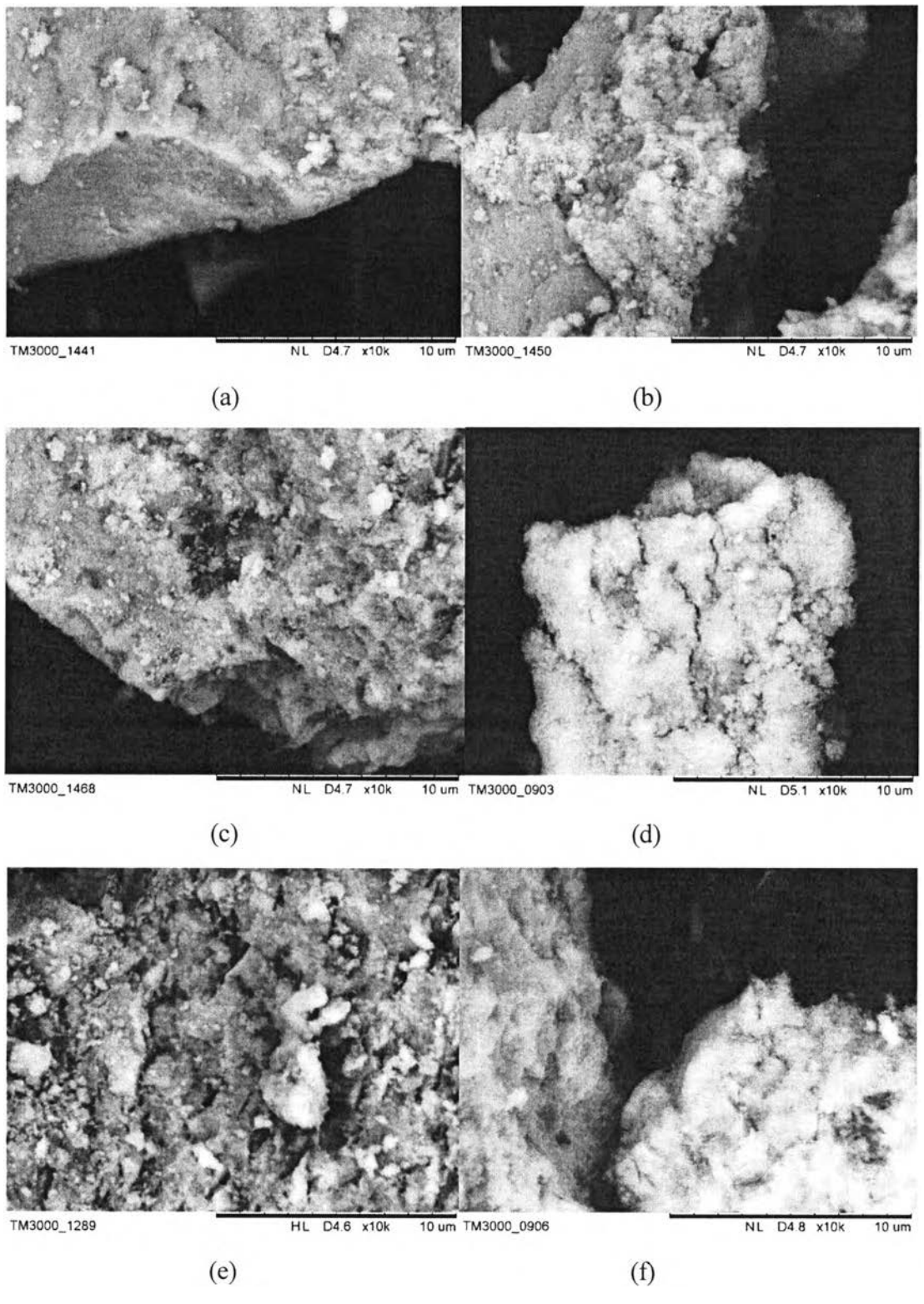

Figure 4.9 SEM images (10000x magnifications) of a) CZO-C, b) Ni/CZO-C, c) CZM-1, d) Ni/CZM-1, e) CZM-2, f) Ni/CZM-2.

All of Mn-doped catalysts illustrate the aggregation of the primary long thin needle shaped particles (Thammachart *et al.*, 2001). The morphology of the individual Ni-doped catalysts was similar to one another depicting the round particles of the NiO particle attached onto the surface of supports. It was shown that both the modified and unmodified CZO by Mg presented a similar morphology of the ceria-zirconia mixed oxide in Figure 4.10. The morphology of the individual Ni-doped catalysts was similar to one another depicting the round particles of the NiO particle attached onto the surface of supports.

4.2 Catalytic Activities for Methane Dry Reforming (MDR)

4.2.1 Catalytic Activities for MDR

The methane dry reforming was carried out over all catalysts under the following conditions: CH_4/CO_2/He molar ratio of 1:1:8, total flow rate 100 ml/min and at atmospheric pressure. All samples contained 15%Ni/CZO with and without modified supports by Mn and Mg to investigate the effect of acid-base properties on the MDR reaction are presented in Figures 4.11-4.15, which include CH_4 conversion, CO_2 conversion, H_2 yield, CO yield, and H_2/CO molar ratio, respectively.

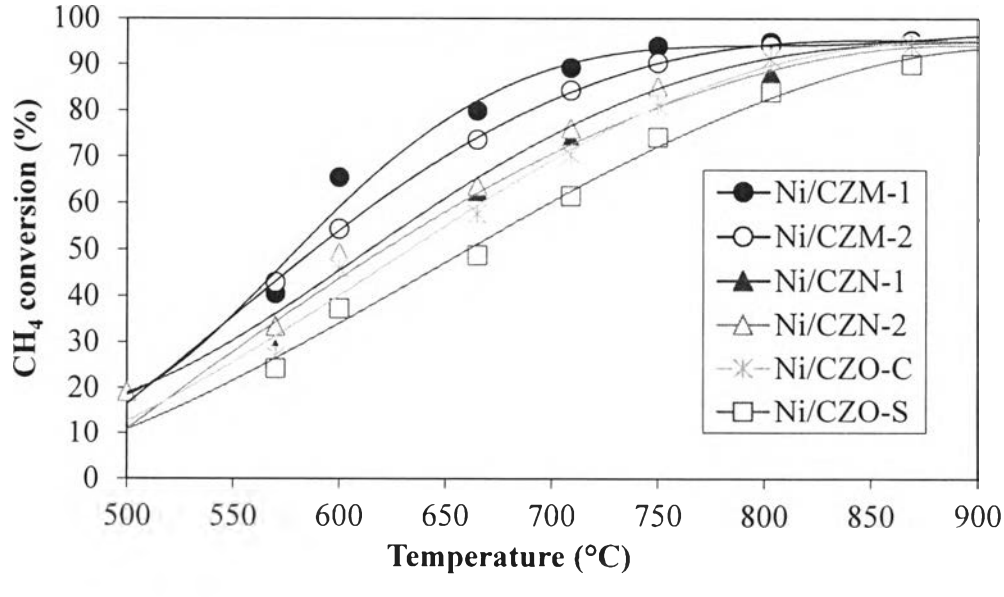

Figure 4.10 CH_4 conversion at different temperatures over the investigated catalysts (CH_4/CO_2/He molar ratio = 1:1:8 and GHSV of 10,600 h^{-1}).

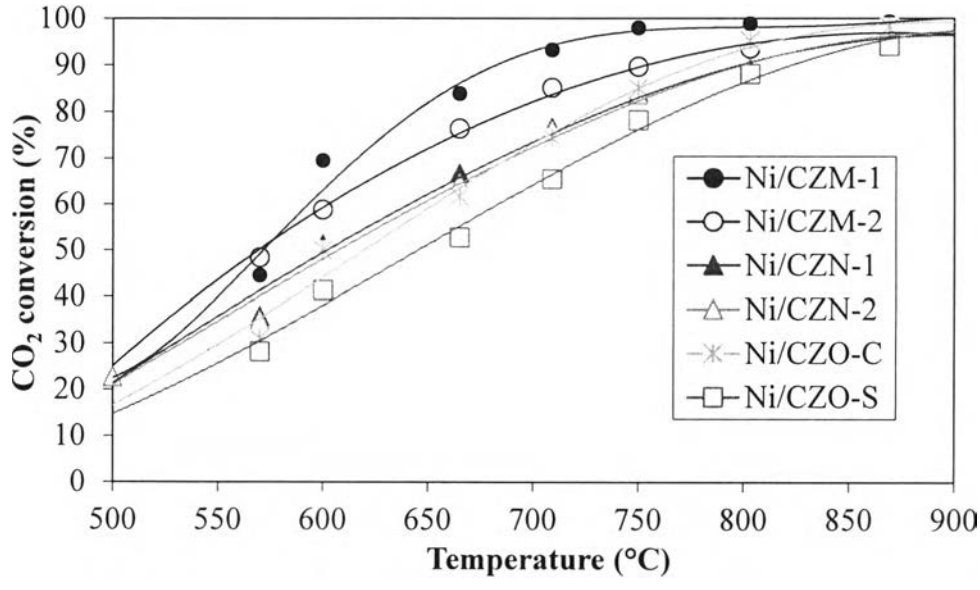

Figure 4.11 CO_2 conversion at different temperatures over the investigated catalysts (CH_4/CO_2/He molar ratio = 1:1:8 and GHSV of 10,600 h^{-1}).

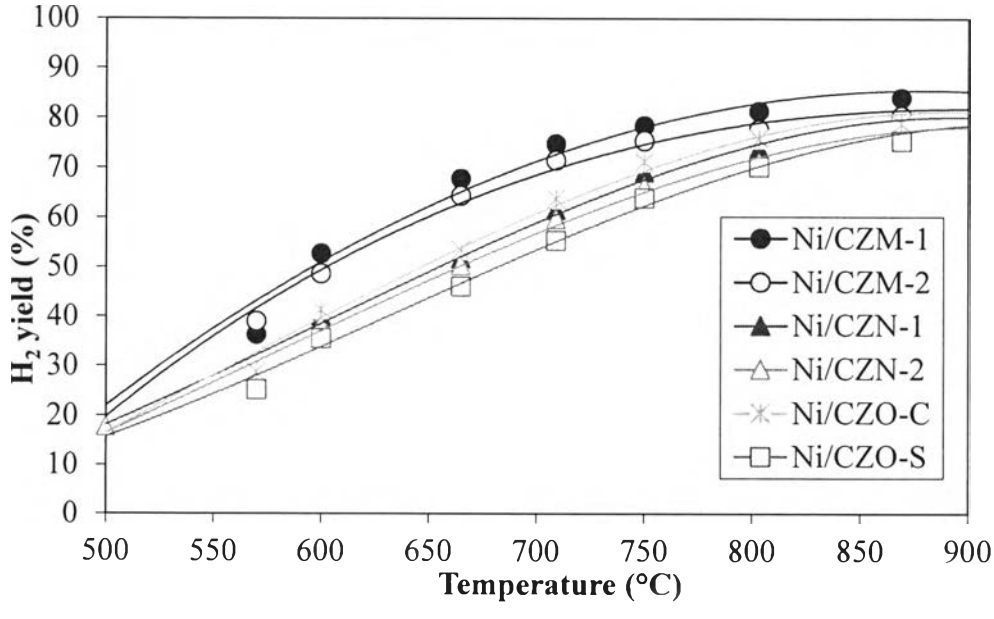

Figure 4.12 H_2 yield at different temperatures over the investigated catalysts (CH_4/CO_2/He molar ratio = 1:1:8 and GHSV of 10,600 h^{-1}).

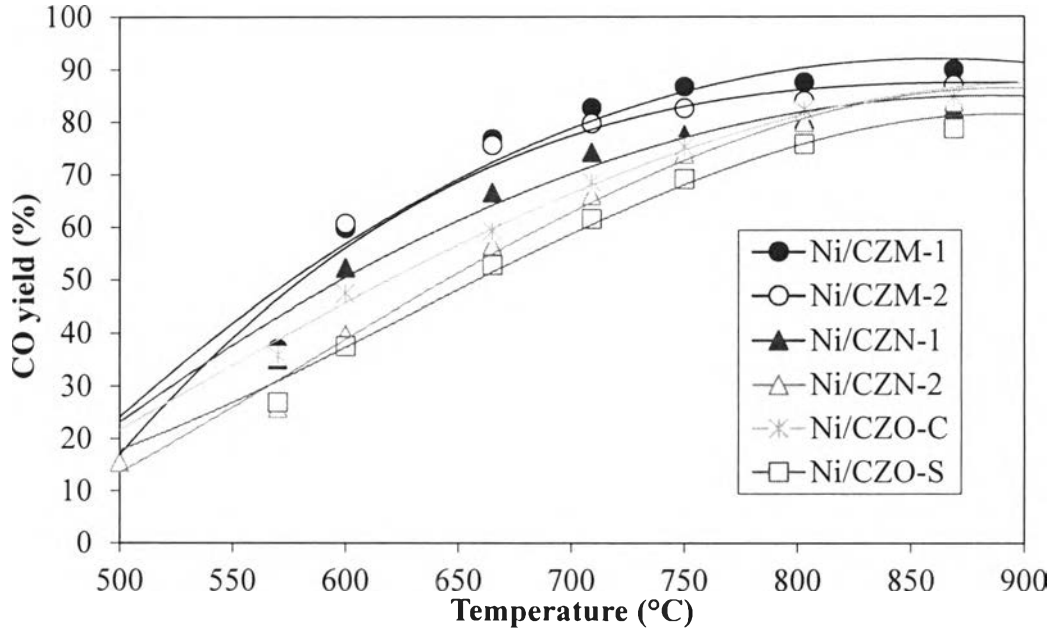

Figure 4.13 CO yield at different temperatures over the investigated catalysts (CH_4/CO_2/He molar ratio = 1:1:8 and GHSV of 10,600 h^{-1}).

The CH_4 and CO_2 conversions increase with increasing temperatures which proved the endothermic property of the MDR reaction ($CH_4 + CO_2 \rightarrow 2H_2 + 2CO$, ΔH = 247.3 kJ/mol). However, it was quite obvious that the CO_2 conversion (X_{CO2}) was higher than the CH_4 conversion (X_{CH4}) in temperatures between 600 and 750 °C. This is due to the occurrence of reverse water gas shift (RWGS) reaction ($H_2 + CO_2 \rightarrow H_2O + CO$, ΔH = -39.5 kJ/mol) and the competition between RWGS and the main MDR reaction which led to increase the conversion of CO_2. This is also resulted CO yield higher than H_2 yield (Albarazi *et al.*, 2013).

The results showed that the modified catalysts (Ni/CZNs and Ni/CZMs) demonstrated more activity catalyst than unmodified catalysts such as Ni/CZOs. In addition Ni/CZO-C catalyst prepared by co-precipitation method was more activity than Ni/CZO-S catalyst prepared by sol-gel method. It was found that surface area of Ni/CZO-C catalyst was higher than Ni/CZO-S catalyst. The Ni/CZM-1 catalyst was found to be the most active catalyst as indicated by CH_4 conversion and CO_2 conversion as shown in Figures 4.11 and 4.12. This is due to its weak metal-support interaction explained by H_2-TPR results

discussed in previous section. On the other hand, the Ni/CZN exhibited lower activity; due to its strong metal support interaction of MDR.

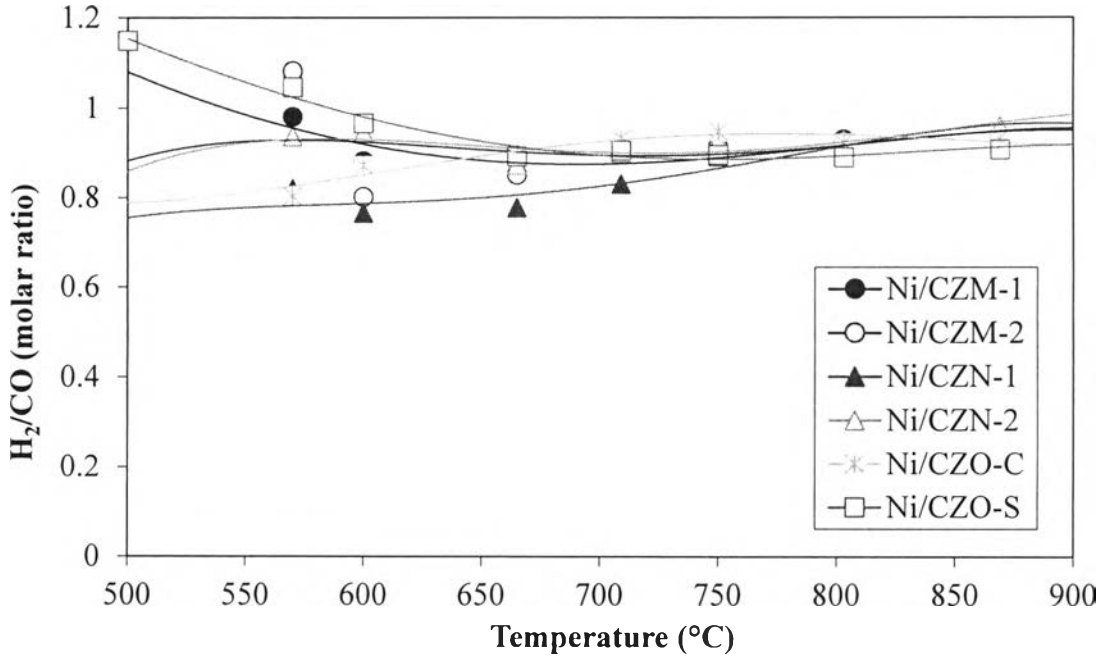

Figure 4.14 H_2/CO molar ratio at different temperatures over the investigated catalysts (CH_4/CO_2/He molar ratio = 1:1:8 and GHSV of 10,600 h^{-1}).

4.4.2 Catalyst Stability

The catalytic stability tests were performed on Ni-doped catalysts under the following conditions: temperature at 750 °C, CH_4/CO_2/He molar ratio of 1:1:8, GHSV of 10,600 h^{-1}, total flow rate 100 ml/min and at atmospheric pressure.

Figures 4.16-4.20 illustrated the CH_4 conversion, CO_2 conversion H_2 and CO yield as well as H_2/CO molar ratio for the investigated catalysts, respectively. Those results showed that the catalysts modified by Mg or Mn showed stable than unmodified catalysts. Apart from Ni/CZN-2, other catalysts are stable throughout 10 h time on stream. The results showed that the reactor was blocked after 5 h for Ni/CZN-2. This is might be due to the fact that Ni/CZN-2 gave the highest acidity which promoted boudouard reaction. In addition to reaction, Ni/CZM-1 catalysts favor main reaction

(MDR) than methane decomposition reaction due to when compared with other catalysts found evidence in the Figures 4.18 and 4.19.

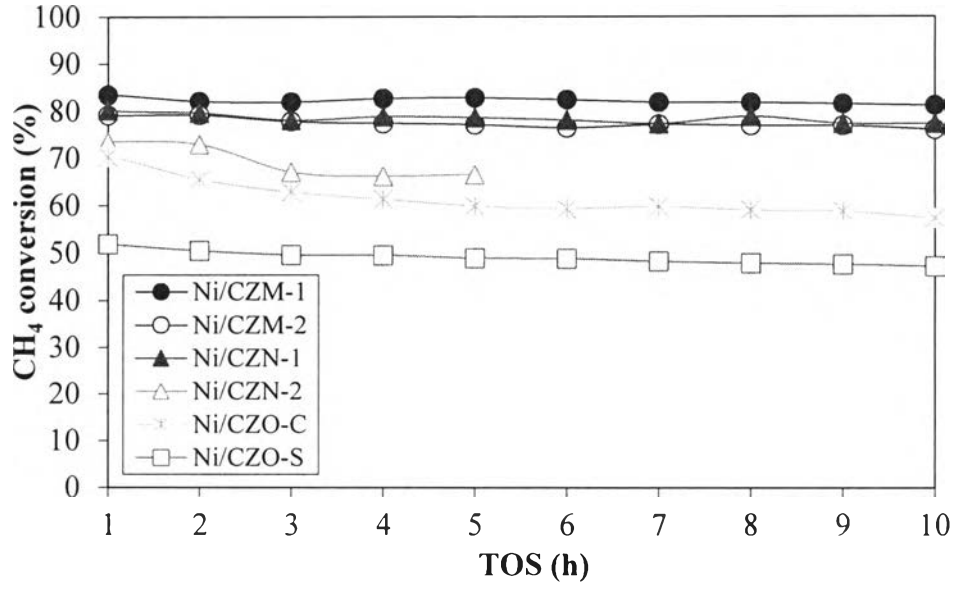

Figure 4.15 CH_4 conversion with time on stream (TOS) over the investigated catalysts at 750 °C (CH_4/CO_2/He molar ratio = 1:1:8 and GHSV of 10,600 h^{-1}).

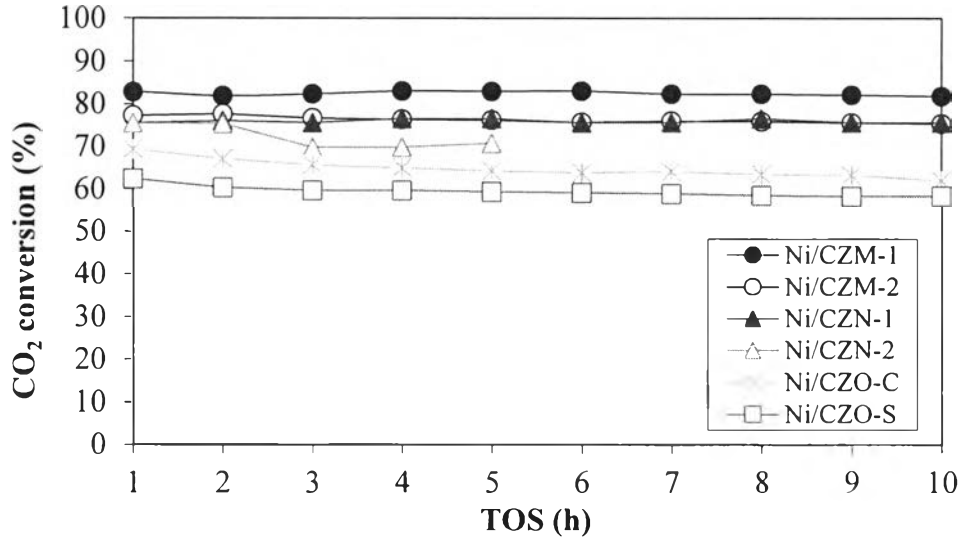

Figure 4.16 CO_2 conversion with time on stream (TOS) over the investigated catalysts at 750 °C (CH_4/CO_2/He molar ratio = 1:1:8 and GHSV of 10,600 h^{-1}).

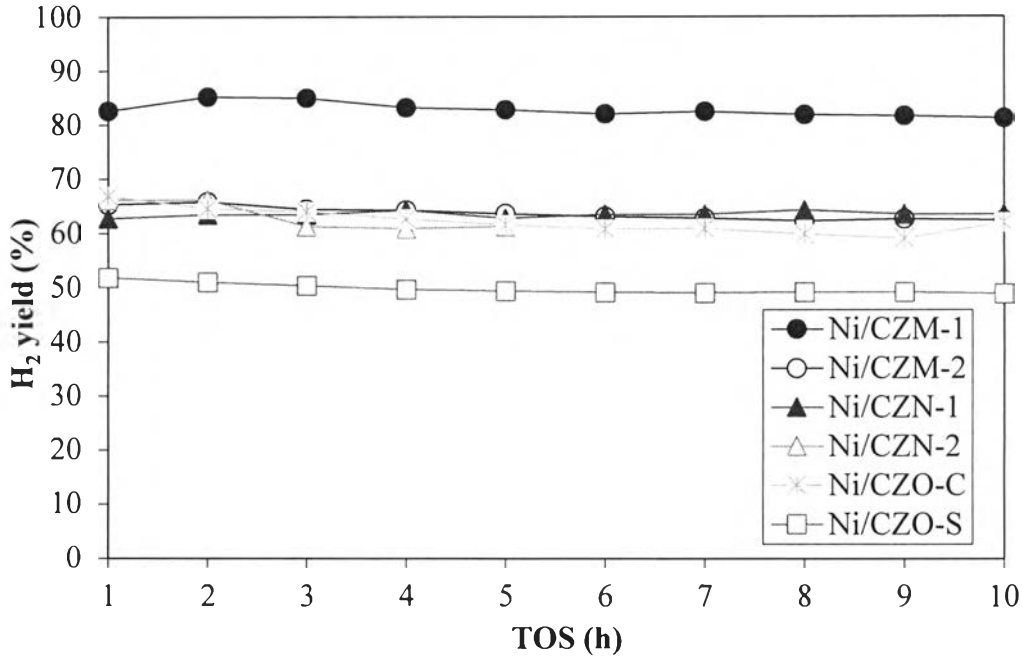

Figure 4.17 H_2 yield with time on stream (TOS) over the investigated catalysts at 750 °C (CH_4/CO_2/He molar ratio = 1:1:8 GHSV of 10,600 h^{-1}).

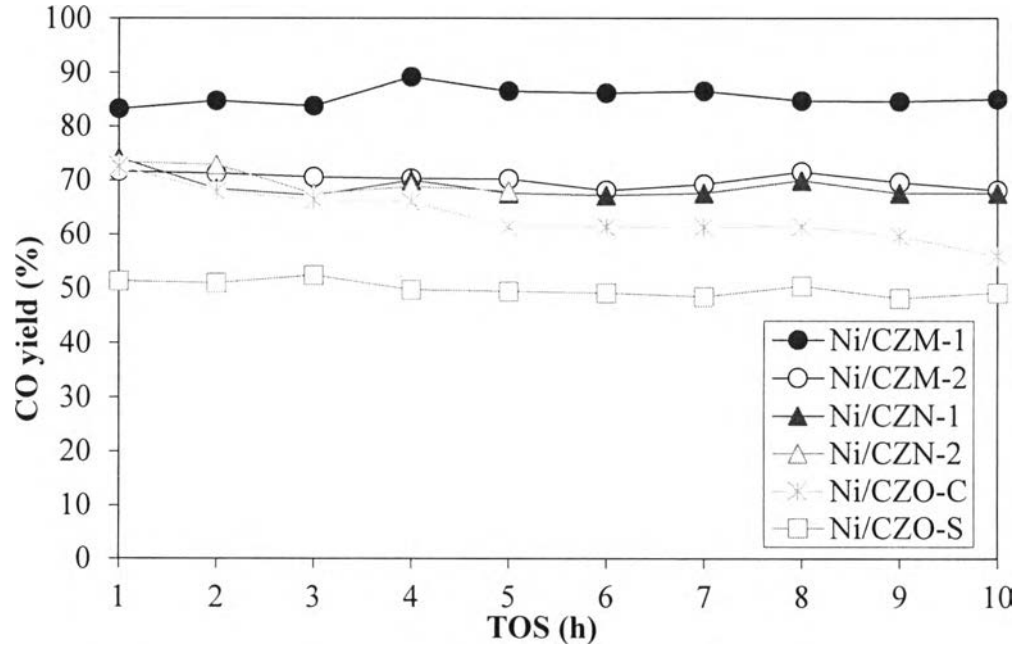

Figure 4.18 CO yield with time on stream (TOS) over the investigated catalysts at 750 °C (CH_4/CO_2/He molar ratio = 1:1:8 and GHSV of 10,600 h^{-1}).

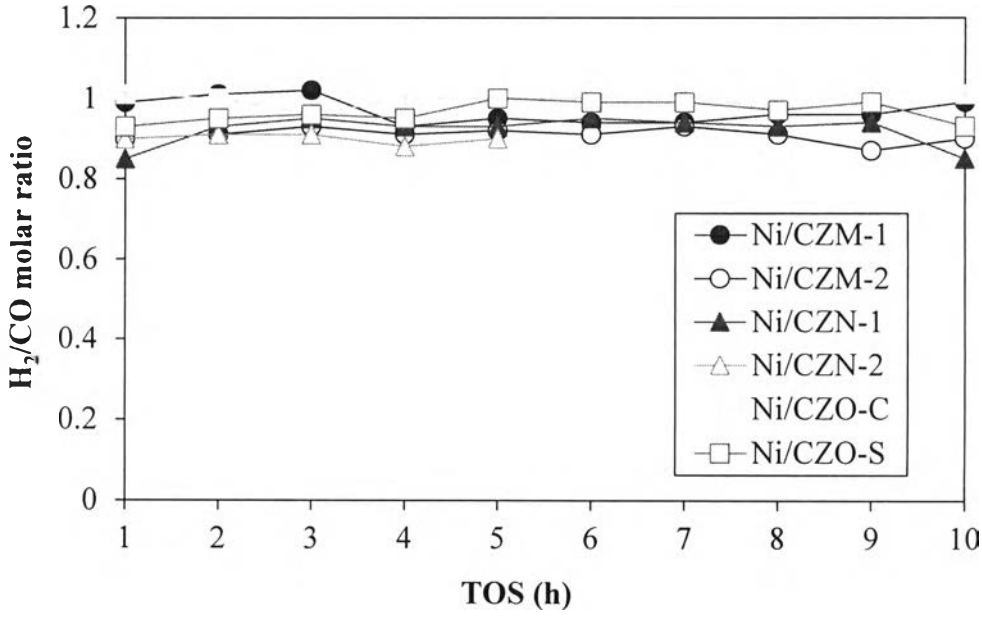

Figure 4.19 H_2/CO molar ratio with time on stream (TOS) over the investigated catalysts at 750 °C (CH_4/CO_2/He molar ratio = 1:1:8 and GHSV of 10,600 h^{-1}).

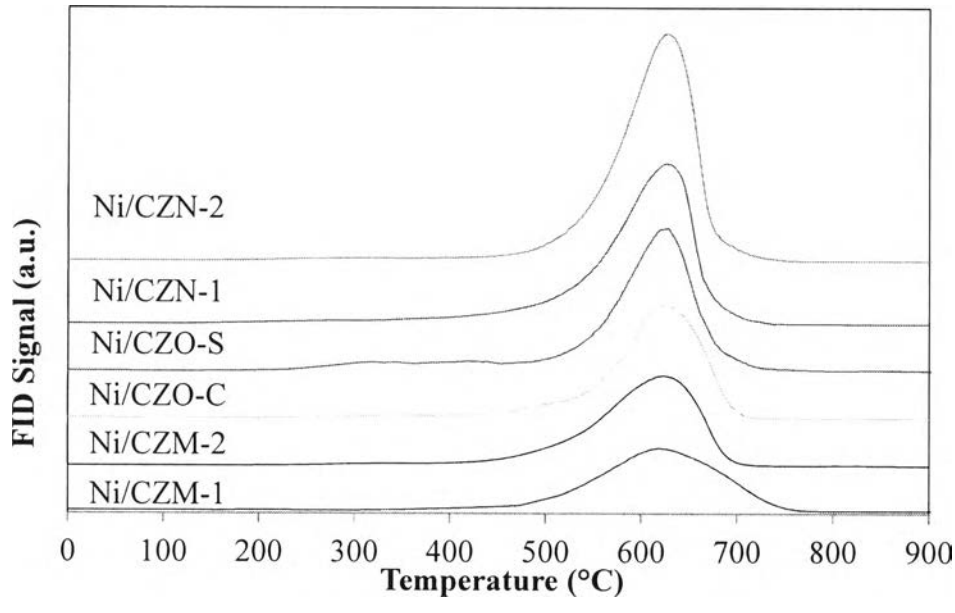

Figure 4.20 TPO profiles of catalysts after reaction at 750 °C (CH_4/CO_2/He molar ratio = 1:1:8 and GHSV of 10,600 h^{-1}) an oxidizing gas containing 2 % O_2 in He with a flow rate of 40 ml/min.

The amounts of carbon deposit on the catalyst after a reaction time of 6 h at 750 °C and CH_4/CO_2/He ratio of 1:1:8 determined by TPO technique are shown in Table 4.2. The amount of coke formation on the Ni/CZO-S spent catalyst was 52 wt% whereas those of coke formation on the Ni/CZN-1, Ni/CZN-2, Ni/CZO-C, Ni/CZM-1 and Ni/CZM-2 spent catalysts were 66, 75, 46, 30, and 35 wt%, respectively. The coke formation was found in the order Ni/CZN > Ni/CZO > Ni/CZM. This results indicated that the Ni/CZM exhibit strong interactions between Ni and support which can prevent the sintering of metal at high temperatures resulting in suppressing the coke formation on the catalysts. It was relevant that the Mg doped into Ce-Zr lattice leads to decrease of number of the strong acid sites improved the basicity of Ni/CZO catalyst which benefited to disfavor the accumulation of carbon on acid sites of support (Milberg *et al.*, 2010).

Table 4.2 Reaction results of stability test at 750°C for 10 h

Catalyst	CH_4 conv. (%)	CO_2 conv. (%)	H_2 yield (%)	CO yield (%)	H_2/CO molar ratio	Amount of coke formation *(wt%)
Ni/CZO-S	49	60	50	50	1.00	52
Ni/CZN-1	73	76	63	69	0.91	66
Ni/CZN-2	68	71	62	69	0.90	75
Ni/CZO-C	62	65	62	64	0.97	46
Ni/CZM-1	82	83	82	86	0.95	30
Ni/CZM-2	72	76	63	69	0.91	35

*TPO technique

The amounts of carbon deposit on the catalyst after a reaction time of 6 h at 750 °C and CH_4/CO_2/He ratio of 1:1:8 determined by TPO technique are shown in Table 4.2. The amount of coke formation on the Ni/CZO-S spent catalyst was 52

wt% whereas those of coke formation on the Ni/CZN-1, Ni/CZN-2, Ni/CZO-C, Ni/CZM-1 and Ni/CZM-2 spent catalysts were 66, 75, 46, 30, and 35 wt%, respectively. The coke formation was found in the order Ni/CZN > Ni/CZO > Ni/CZM. This results indicated that the Ni/CZM exhibit strong interactions between Ni and support which can prevent the sintering of metal at high temperatures resulting in suppressing the coke formation on the catalysts. It was relevant that the Mg doped into Ce-Zr lattice leads to decrease of number of the strong acid sites improved the basicity of Ni/CZO catalyst which benefited to disfavor the accumulation of carbon on acid sites of support (Milberg *et al.*, 2010).